A magnetic resonance imaging-based prognostic scoring system to predict outcome in transplant-eligible patients with multiple myeloma

Elias K. Mai,[1] Thomas Hielscher,[2] Jost K. Kloth,[3] Maximilian Merz,[1] Sofia Shah,[1] Marc S. Raab,[1] Michaela Hillengass,[1] Barbara Wagner,[1] Anna Jauch,[4] Dirk Hose,[1] Marc-André Weber,[3] Stefan Delorme,[5] Hartmut Goldschmidt,[1] and Jens Hillengass[1]

[1]Department of Internal Medicine V, University Hospital of Heidelberg; [2]Division of Biostatistics, German Cancer Research Center; [3]Department of Diagnostic and Interventional Radiology, University Hospital of Heidelberg; [4]Institute of Human Genetics, University of Heidelberg; and [5]Department of Radiology, German Cancer Research Center, Heidelberg, Germany

ABSTRACT

Diffuse and focal bone marrow infiltration patterns detected by magnetic resonance imaging have been shown to be of prognostic significance in all stages of monoclonal plasma cell disorders and have, therefore, been incorporated into the definition of the disease. The aim of this retrospective analysis was to develop a rapidly evaluable prognostic scoring system, incorporating the most significant information acquired from magnetic resonance imaging. Therefore, the impact of bone marrow infiltration patterns on progression-free and overall survival in 161 transplant-eligible myeloma patients was evaluated. Compared to salt and pepper/minimal diffuse infiltration, moderate/severe diffuse infiltration had a negative prognostic impact on both progression-free survival (P<0.001) and overall survival (P=0.003). More than 25 focal lesions on whole-body magnetic resonance imaging or more than seven on axial magnetic resonance imaging were associated with an adverse prognosis (progression-free survival: P=0.001/0.003 and overall survival: P=0.04/0.02). A magnetic resonance imaging-based prognostic scoring system, combining grouped diffuse and focal infiltration patterns, was formulated and is applicable to whole-body as well as axial magnetic resonance imaging. The score identified high-risk patients with median progression-free and overall survival of 23.4 and 55.9 months, respectively (whole-body-based). Multivariate analyses demonstrated that the magnetic resonance imaging-based prognostic score stage III (high-risk) and adverse cytogenetics are independent prognostic factors for both progression-free and overall survival (whole-body-based, progression-free survival: hazard ratio=3.65, P<0.001; overall survival: hazard ratio=5.19, P=0.005). In conclusion, we suggest a magnetic resonance imaging-based prognostic scoring system which is a robust, easy to assess and interpret parameter summarizing significant magnetic resonance imaging findings in transplant-eligible patients with multiple myeloma.

Introduction

Although the vast majority of patients with multiple myeloma (MM) remains incurable, their median survival has improved markedly thanks to the introduction of high-dose chemotherapy in combination with novel agents such as proteasome inhibitors and immunomodulatory drugs.[1,2] Currently accepted prognostic scores predicting progression-free survival (PFS) and overall survival (OS) of newly diagnosed MM patients are based on laboratory values, namely the International Staging System (ISS),[3] cytogenetic analyses[4,5] or combinations of both.[6,7] None of these includes imaging criteria so far. Cytogenetic aberrations will reflect the molecular biology of the malignant cells, and laboratory results mainly their secretory activity and indirectly the tumor mass. Imaging findings, especially when using dedicated whole body protocols in magnetic resonance imaging (wbMRI) and positron emission computed tomography (PET-CT), may help to estimate the total burden of tumor cells in the bone marrow. Furthermore, MRI can depict the spatial distribution of tumor cells, which might reflect some of their biological as well as disease features.[8–11]

MRI in particular is progressively being used in clinical routine in accordance with the current diagnostic guidelines of the International Myeloma Working Group (IMWG).[11–13] Furthermore, MRI findings have recently been incorporated in the revised IMWG criteria to define symptomatic MM, which makes it necessary to perform MRI at baseline for patients who do not fulfill the classical CRAB criteria.[14] Different bone marrow infiltration patterns, such as focal lesions (FL), diffuse infiltration (DI), including a so-called salt and pepper pattern (S&P), can be detected.[12,15]

In symptomatic MM, the presence of more than seven FL in axial MRI (axMRI) is associated with a shorter OS.[9] In asymptomatic stages of monoclonal plasma cell diseases, more than one FL as well as progression of a FL or DI over time have been shown to be associated with a higher risk of progression into symptomatic disease.[16–18] Patterns of DI are associated with high-risk cytogenetics and with a poor prognosis.[8,10,19]

Extracting the significant information provided by MRI studies is demanding for both the radiologist and the hematologist. However, a prognostic score which combines different information delivered by MRI might help to summarize the available findings in a systemic fashion and make them interpretable and comparable for the treating physician. The

 doi:10.3324/haematol.2015.124115
The online version of this article has a Supplementary Appendix.
Manuscript received on January 19, 2015. Manuscript accepted on March 11, 2015.
Correspondence: jens.hillengass@med.uni-heidelberg.de

present study was aimed at analyzing the different MRI patterns in order to develop and suggest a MRI-based prognostic scoring system (MPSS) for transplant-eligible MM patients.

Methods

Subjects

We retrospectively assessed the wbMRI of 161 previously untreated transplant-eligible MM patients from our institution. Patients were included in the present analysis if wbMRI had been performed within 90 days before the initiation of systemic chemotherapy between October 2004 and March 2010 (median 20 days; range, 0 - 87 days) and if at least one autologous stem cell transplant had been part of the first-line treatment. The baseline characteristics of the patients and MRI features are shown in *Online Supplementary Table S1*. Sixty-seven patients had induction therapy without novel agents, 24 patients had an induction therapy including thalidomide, and 70 patients had an induction therapy including bortezomib. Ninety patients underwent single melphalan high-dose (200 mg/m^2) therapy and autologous blood stem cell transplantation, while 69 patients underwent tandem high-dose melphalan and autologous stem cell transplantation. Maintenance therapy was administered to 82 patients, of whom 46 were given thalidomide, 19 bortezomib and 17 interferon. Retrospective data analysis was approved by the institutional ethics committee (Heidelberg, S247/2012).

Imaging protocol and analysis

Whole-body MRI was conducted as previously described, without the administration of a contrast agent, on two similar 1.5 Tesla MRI scanners.[18,20,21] Two investigators analyzed the images in consensus reading. Briefly, FL are circumscriptive lesions (>5 mm in diameter) that are hypointense in T1w and hyperintense in T2w images.[15] The FL were counted and the numbers of intra-axial (spine and sacral bone) and extra-axial lesions were recorded separately. In general, DI is defined by a homogeneous decrease of signal intensity in T1w and a homogeneous increase of signal intensity in T2w images. In our study, DI was divided into three grades of severity according to Baur and Staebler[22,23] as follows: normal/minimal DI of the bone marrow was defined by a hyperintense signal in T1w images and low signal intensity on short-tau inversion recovery (STIR) images. Moderate DI was defined as a decrease in T1w signal intensity of the bone marrow which was, however, still higher than the signal of the intervertebral discs. A decrease of the signal intensity as low as that of the intervertebral discs (or even lower) in T1w images was graded as severe DI. The S&P pattern was defined as a heterogeneous patchy bone marrow pattern.[23] Exemplary T1w MRI images of the different patterns of infiltration are shown in *Online Supplementary Figure S1*.

Cytogenetic analysis

Cytogenetic analyses were performed according to standardized local procedures using interphase fluorescence *in-situ* hybridization (iFISH).[5] High-risk cytogenetics were defined as a 17p deletion and/or 4;14 translocation and/or gain of 1q21 (>3 copies) as previously described.[5]

Statistical analyses

PFS was defined as time from MRI to progression or death from any cause, whichever occurred first. OS was defined as time from MRI to death from any cause. Patients without events were censored at last follow-up. The distribution of event times was estimated using the Kaplan-Meier method. The log-rank test was used to compare survival curves. For MPSS, the log-rank trend test with ordered alternative hypotheses was used and subsequent pairwise comparisons were adjusted for multiple testing.[24] Cox regression was used to assess the prognostic impact of variables. For multivariate Cox regression, multiple imputation (B=100) of missing values was performed using the predictive mean matching algorithm[25] as implemented in R package Hmisc. All tests were two-sided. *P* values less than 0.05 were considered statistically significant. All analyses were performed using R 3.1 (R Core Team, *http://www.R-project.org/*).

Results

Impact of focal and diffuse magnetic resonance imaging patterns on progression-free and overall survival

The median follow-up was 64 months and data were last updated in January 2014. There were 123 PFS and 49 OS events. PFS and OS for S&P, minimal, moderate and severe DI were significantly different (PFS: $P<0.001$ and OS; $P=0.01$, respectively, Figure 1A,B). Grouping these patterns into S&P/minimal DI and moderate/severe DI also revealed significant differences for PFS and OS (PFS: $P<0.001$ and OS: $P=0.003$) (Figure 1C,D).

The analysis of the MRI FL revealed that a higher number of FL was associated with a continuously increasing risk of shortened PFS and OS (*Online Supplementary Figure S2A,B*). There was no unique cut-off number of FL to distinguish patients at lower or higher risk. We, therefore, used a distribution-based cut-off of FL number at the third quartile (Q3, approximately 25% of patients with the highest numbers of FL) to define patients at a high risk. In this cohort, the third quartile using wbMRI was 25 FL while it was seven FL when only counting axial FL. PFS and OS were significantly different when these cut-offs were applied (PFS: wbFL $P=0.001$, axFL $P=0.004$ and OS: wbFL $P=0.04$, axFL $P=0.02$, respectively, Figure 2A-D).

The univariate Cox proportional hazards analysis identified the grouped DI patterns (moderate/severe *versus* S&P/minimal) as risk factors for shortened PFS and OS [DI moderate/severe: hazard ratio (HR)=2.10, $P<0.001$ for PFS and HR=3.00, $P=0.005$ for OS, respectively). This was also seen for the third quartile FL cut-offs (wbFL >25/axFL >7: HR=1.90/1.82, $P=0.002/0.004$ for PFS and HR=1.89/2.00, $P=0.04/0.03$ for OS, respectively). Other known prognostic parameters such as adverse cytogenetics (HR=1.85, $P=0.001$ for PFS and HR 2=55, $P=0.004$ for OS), lactate dehydrogenase (LDH) [> upper limit of normal (ULN), HR=2.59, $P=0.002$ for OS] and ISS stage III (HR=1.92, $P=0.007$ for PFS and HR=3.29, $P<0.001$ for OS) were linked to adverse PFS and OS in our cohort. The results of univariate analyses are shown in *Online Supplementary Table S2*.

Multivariate Cox proportional hazards analyses were performed to evaluate the prognostic impact of grouped DI patterns and FL MRI cut-offs on PFS and OS (Table 1). The model was calculated using either wbFL/MRI (Table 1, top) or axFL/MRI (Table 1, bottom). The wbFL (>25) as well as axFL (>7) remained significant independent prognostic risk factors in these analyses (PFS: wbFL, HR=2.00, $P=0.002$; axFL, HR=2.12, $P=0.001$ and OS: wbFL HR=2.21, $P=0.02$; axFL, HR=2.45, $P=0.01$, respectively). In both mul-

tivariate models, the grouped DI pattern (moderate/severe) had a significant effect on the prognosis (PFS: wbMRI, HR=1.80, *P*=0.01; axMRI, HR=1.90, *P*=0.005 and OS: wbMRI HR=2.31, *P*=0.04; axMRI, HR=2.60, *P*=0.02). The multivariate analysis also confirmed that adverse cytogenetics remained independent prognostic risk factors for adverse PFS and OS (wbMRI: PFS, HR=1.66, *P*=0.02 and OS: HR=2.07, *P*=0.04; axMRI: PFS, HR=1.62, *P*=0.02 and OS, HR 1.97, *P*=0.05/not significant, respectively). LDH (>ULN, axMRI: OS: HR=1.96, *P*=0.04) remained a significant predictor for adverse OS in the axMRI multivariate model (Table 1).

The magnetic resonance imaging-based prognostic scoring system combining focal and diffuse magnetic resonance imaging patterns

Since both the grouped diffuse and focal MRI patterns had a significant impact on PFS and OS in univariate and multivariate models, the combination of the grouped MRI patterns appeared appropriate.

To create an MRI-based scoring system (MPSS) for transplant-eligible MM, three stages were defined: stage I included patients with S&P/minimal DI MRI and 0-25 wbFL (or 0-7 axFL). Stage II was defined as either S&P/minimal DI MRI and >25 wbFL (or >7 axFL) or moderate/severe DI MRI and 0-25 wbFL (or 0-7 axFL). Stage III was defined as moderate/severe DI MRI and >25 wbFL (or > 7 axFL).

When applying the wb-MPSS to our cohort, 23.6% of the patients would be in stage I, 59.6% in stage II and 16.8% in stage III. If the ax-MPSS was applied, 22.4% of the patients were allocated to stage I, 64.0% to stage II and 13.6% to stage III. There were no major changes in the composition of the MPSS when using either the wbFL or axFL cut-offs (*Online Supplementary Table S3*).

The classification according to the MPSS and the 3-year PFS and 5-year OS rates (%) when using either wbMRI or

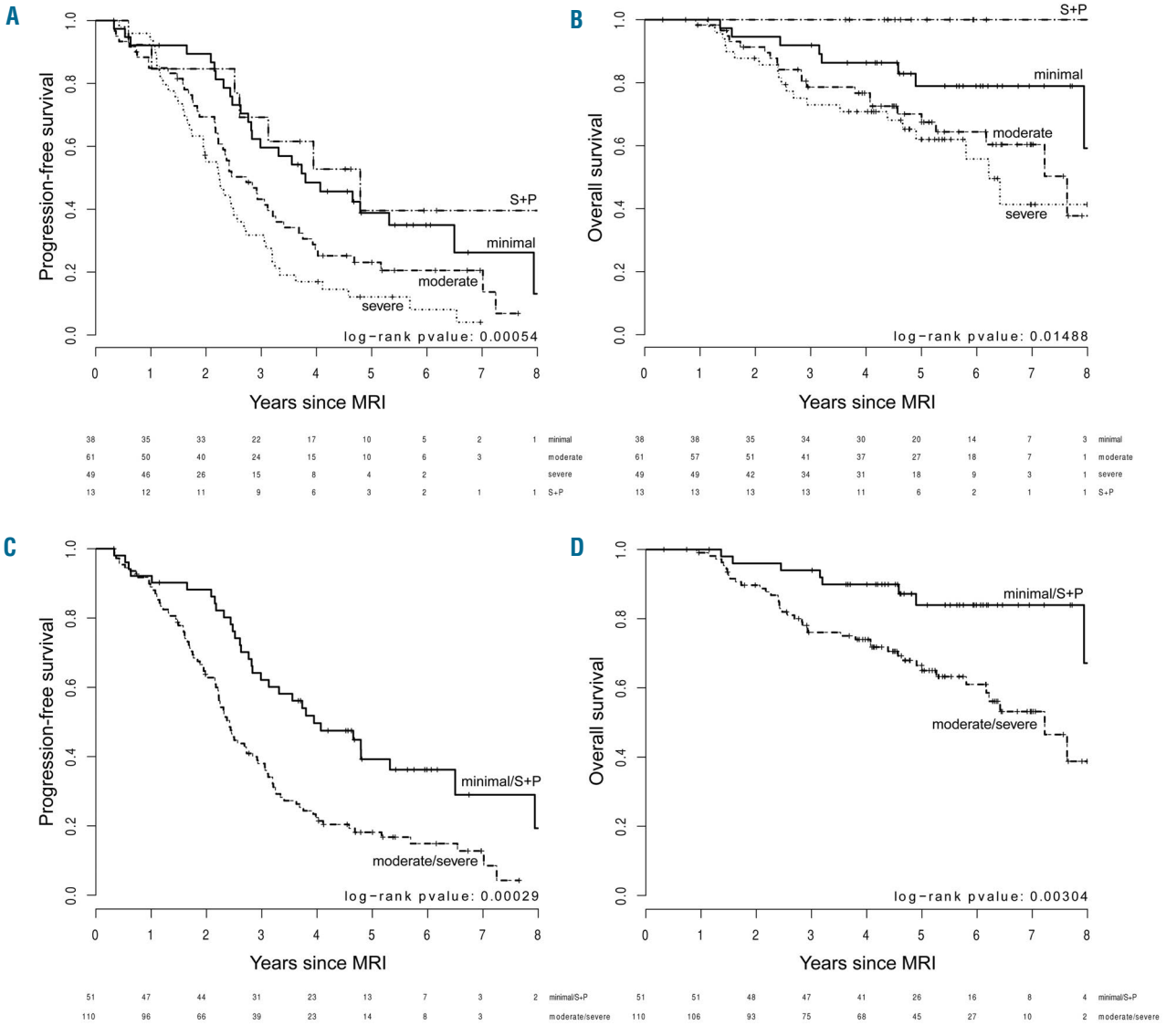

Figure 1. Kaplan-Meier plots of diffuse MRI patterns. (A, B) PFS and OS for the different MRI patterns: salt and pepper (S&P), minimal, moderate, and severe diffuse infiltration. (C, D) PFS and OS for the grouped diffuse MRI patterns S&P/minimal and moderate/severe.

axMRI are shown in Table 2. MPSS stage III defined patients at the highest risk of early progression with a median PFS of 23.4 months (wb-MPSS) and 26.0 months (ax-MPSS). Concomitantly, the median survival for patients in stage III was 55.9 months (wb-MPSS) and 48.9 months (ax-MPSS). The median PFS for MPSS stage I and II patients were 57.5 (wb-MPSS) and 63.8 months (ax-MPSS) months and 31.3 (wb-MPSS) and 30.0 (ax-MPSS) months, respectively. The median survival was not reached in patients with either wb-MPSS or ax-MPSS stage I and was 86.8 months (wb-MPSS) and not reached (ax-MPSS) in patients in MPSS stage II.

Both the wb-MPSS and the ax-MPSS were able to reliably distinguish PFS and OS for the three different stages. With the exception of the discrimination between stage II and III when using the wb-MPSS (borderline significance, P=0.05, Figure 3B), all pair-wise multiplicity-adjusted log-rank tests between the defined wb-MPSS and ax-MPSS, were statistically significant (Figure 3A-D).

The wb-MPSS and ax-MPSS were then incorporated into a multivariate Cox proportional hazards model to evaluate their prognostic impact on PFS and OS (Table 3). In this analysis, MPSS stages II and III were independent, highly significant prognostic parameters for PFS (wb-MPSS stage II/III: HR=2.19/3.65, P=0.003/<0.001 and ax-MPSS stage II/III: HR=2.27/3.95, P=0.002/<0.001, respectively) together with adverse cytogenetics (wb-/ax-MPSS model: HR=1.60/1.59, P=0.02/0.02). The multivariate analysis further demonstrated that MPSS stage III (wb-/ax-MPSS: HR=5.19/5.73, P=0.005/0.003) and adverse cytogenetics (wb-/ax-MPSS model: HR=2.07/2.01, P=0.04/0.04) were the only consistent independent predictors for adverse OS in both models. Known prognostic parameters such as ISS stage III, LDH (>ULN) and induction therapy including novel agents were close to being statistically significant (Table 3).

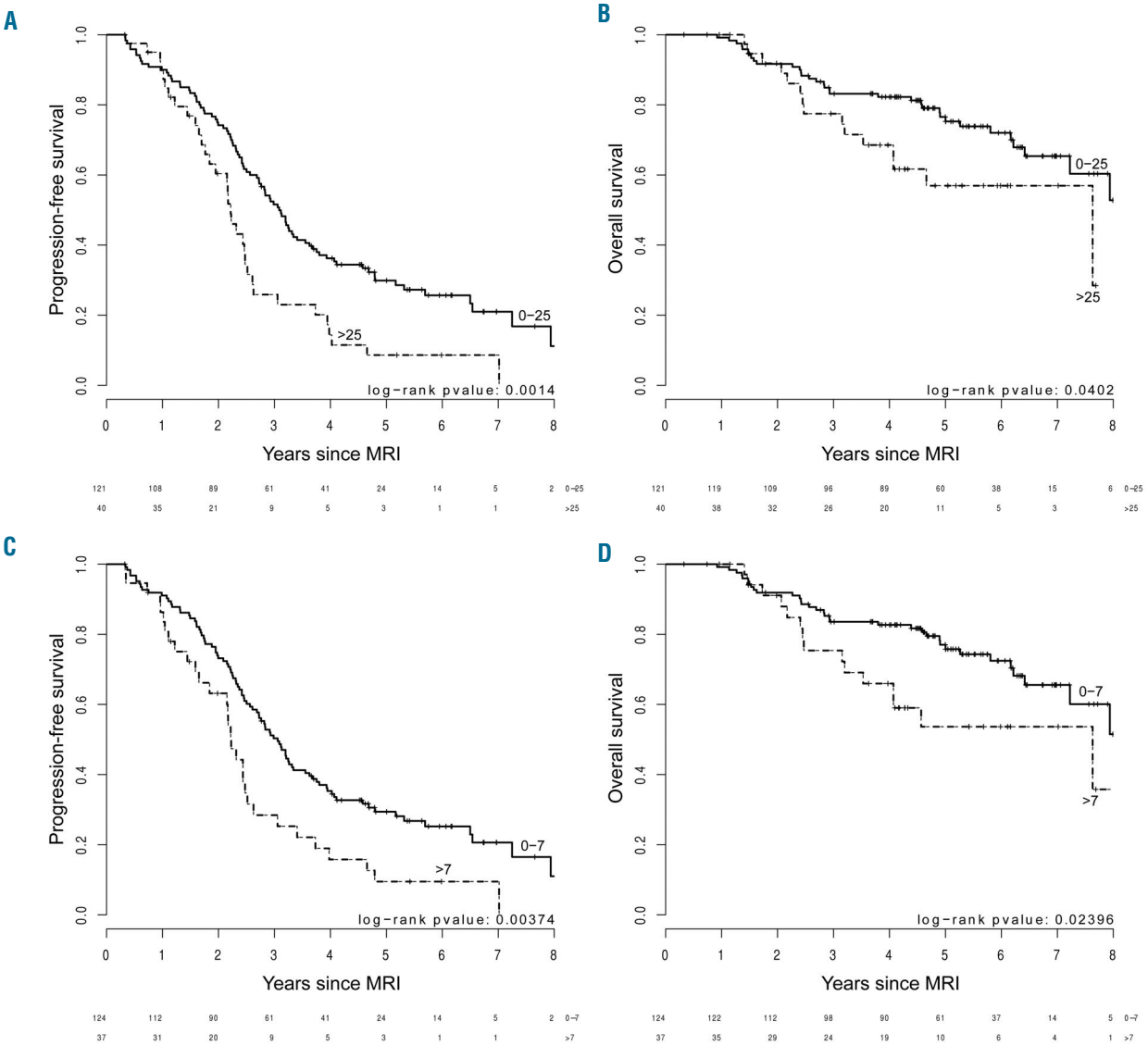

Figure 2. Kaplan-Meier plots of focal MRI patterns. (A, B) PFS and OS according to number of FL on wbMRI (0-25 *vs.* >25). (C, D) PFS and OS according to number of FL on axMRI (0-7 *vs.* >7).

Table 1. Multivariate model of the impact of MRI patterns and described prognostic factors on PFS and OS. The model was calculated using either the cut-off for whole-body MRI focal lesions (top) or axial MRI focal lesions (bottom).

	Whole-body MRI-based model					
Parameter	HR	PFS 95%-CI	*P* value	HR	OS 95%-CI	*P* value
MRI wbFL (>25 *vs.* 0-25)	2.00	1.30 – 3.08	0.002	2.21	1.13 – 4.34	0.02
MRI DI (moderate/severe *vs.* normal/S&P)	1.80	1.16 – 2.79	0.01	2.31	1.04– 5.17	0.04
ISS (II *vs.* I)	1.11	0.68 – 1.81	0.67	0.75	0.33 – 1.69	0.48
ISS (III *vs.* I)	1.42	0.85 – 2.37	0.18	1.98	0.97 – 4.06	0.06
LDH (>ULN)	1.04	0.66 – 1.64	0.87	1.79	0.95 – 3.39	0.07
Adverse cytogenetics	1.66	1.10 – 2.49	0.02	2.07	1.05 – 4.10	0.04
Induction therapy without novel agents	1.03	0.71 - 1.50	0.87	1.80	0.98 - 3.31	0.06
	Axial MRI-based model					
Parameter	HR	PFS 95%-CI	*P* value	HR	OS 95%-CI	*P* value
MRI axFL (>7 *vs.* 0-7)	2.12	1.34 – 3.36	0.001	2.45	1.22 – 4.90	0.01
MRI DI (moderate/severe *vs.* normal/S&P)	1.90	1.22 – 2.96	0.005	2.60	1.14– 5.93	0.02
ISS (II *vs.* I)	1.18	0.72 – 1.92	0.51	0.76	0.34 – 1.73	0.51
ISS (III *vs.* I)	1.28	0.75 – 2.19	0.36	1.80	0.85 – 3.80	0.12
LDH (>ULN)	1.11	0.70 – 1.77	0.65	1.96	1.03 – 3.76	0.04
Adverse cytogenetics	1.62	1.07 – 2.44	0.02	1.97	1.00 – 3.89	0.05
Induction therapy without novel agents	0.97	0.66 - 1.41	0.86	1.69	0.93 - 3.07	0.08

Discussion

The adverse prognostic value of DI and FL in MRI has been demonstrated in all stages of monoclonal plasma cell disease as well as in different cohorts of patients.[9,12,13,19] MRI findings have, therefore, recently been incorporated into the revised criteria to define symptomatic MM.[14] However, to date the significance of the combination of the key information acquired from MRI, i.e. number of FL and degree of DI, has not been evaluated.

In the present retrospective study we confirmed that both DI and FL, determined by MRI, have an important impact on PFS and OS. We combined these MRI patterns for the first time to create a MPSS for newly diagnosed, transplant-eligible MM patients. The MPSS is able to identify patients with a poor PFS and OS and was proven independent as a prognostic risk indicator in our subsequent multivariate analyses.

The DI and FL determined by MRI have been shown to correlate with different growth patterns found in histology[26] and therefore appear to be of pathophysiological significance. Several studies established the adverse prognostic significance of DI in MRI.[8,10,19] It is, however, difficult for a reader to differentiate reliably between moderate and severe DI, since there is no objective measure for the signal intensity of the bone marrow. Furthermore, delayed fatty conversion of normal bone marrow in middle-aged patients as well as reactive changes are possible sources of error.[27] It must also be noted that FL may be difficult to delineate if they lie within a diffusely infiltrated bone marrow. While our study confirmed previous findings on the prognostic significance of DI overall, we also found a favorable prognostic implication of a micro-nodular/S&P DI, which had not yet been described in a large cohort (Figure 1). Indeed, we saw that this distinct pattern has the same prognostic significance as a minimal infiltration appearing as a "normal" image in MRI. Furthermore, we demonstrated that moderate and severe DI do not have a significantly different prognostic value.[22] We, therefore, think that a differentiation between homogeneous DI (i.e. moderate and severe) and minimal/normal together with S&P may be sufficient.

Table 2. The MRI-based prognostic score (MPSS) for multiple myeloma.

Stage	MRI characteristics			3-year PFS (%)	5-year OS (%)
	wbFL	or axFL	DI		
I	0-25	0-7	normal/S&P	wb: 71 ax: 72	wb: 87 ax: 86
II	0-25 >25	0-7 >7	moderate/severe normal/S&P	wb: 41 ax: 41	wb: 72 ax: 74
III	>25	>7	moderate/severe	wb: 22 ax: 23	wb: 47 ax: 33

The number of MRI FL has a notoriously adverse impact on PFS and OS. A study conducted by Walker *et al.*,[9] using ax MRI, identified more than seven FL as an independent adverse factor for event-free survival and OS. Of the 611 patients in that study, 211 (~ 36%) had more than seven FL on ax MRI.[9]

A relative hazard analysis based on a Cox model revealed a continuously increasing risk for adverse PFS and OS depending on the number of FL (*Online Supplementary Figure S2*). Although the prognosis became progressively and continuously worse with the number of FL, our search for an optimal cut-point did not reveal a unique cut-off point in our cohort (*data not shown*). This led to the conclusion that no unique cut-off between low and high-risk patients could be made based on the number of FL. We, therefore, decided to choose a distribu-

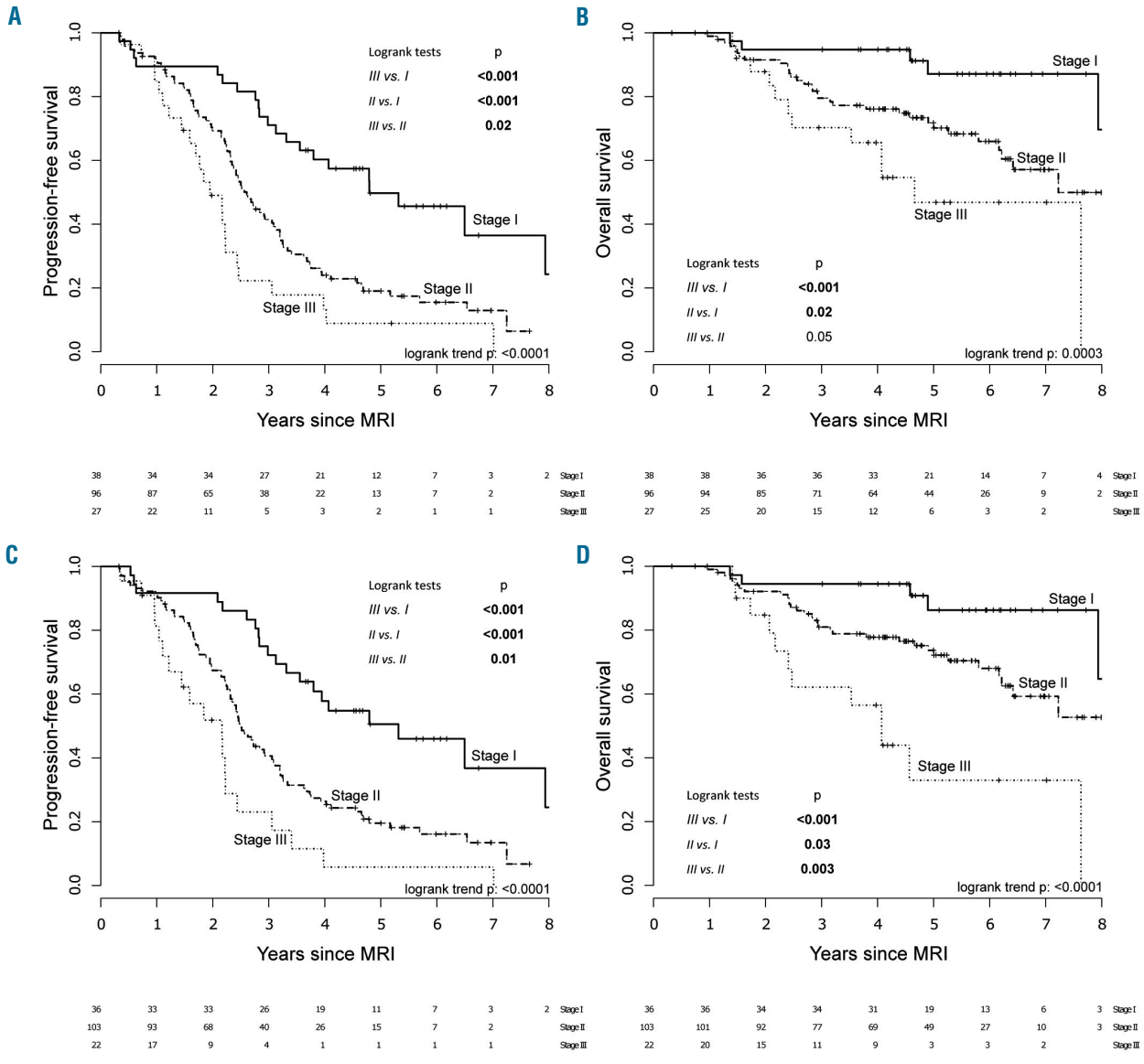

Figure 3. Kaplan-Meier plots of the MRI-based prognostic score (MPSS). (A, B) PFS and OS for the MPSS using the wbMRI FL cut-off (0-25 and >25). (C, D) PFS and OS for the MPSS using the axMRI FL cut-off (0-7 and >7).

tion-based cut-off at the third quartile (representing approximately 25% of all patients). This cut-off was set at >25 FL for wbMRI and >7 for axMRI in our cohort (Figure 2). The latter cut-off was in line with the previous studies by Walker *et al.*, who performed axMRI as described above.[9]

While DI is best identified in the spine or pelvis and wbMRI is not, therefore, mandatory to acquire this information, a comparative study of wbMRI and axMRI revealed that about 10% of patients show FL exclusively outside the axial skeleton.[21] However, since wbMRI is not available in all institutions, we decided to calculate the cut-offs for wbMRI as well as for axMRI and provide results for both. Whether wbMRI will be required or spinal/axial MRI may be sufficient in patients with monoclonal plasma cell diseases will have to be evaluated in future studies. Notably, CT, if performed additionally, is valid for detecting both focal and diffuse disease in the appendicular skeleton, at least in the shafts of long bones.

In our multivariate analysis, FL cut-offs as well as the moderate/severe DI pattern remained significant independent prognostic factors for PFS and OS together with adverse cytogenetics (Table 1), as previously reported.[8,9,22] Other known prognostic factors, such as an elevated LDH, ISS stage III and induction therapy with novel agents, however, often did not reach statistical significance. Although it has been described that ISS and LDH have a stronger impact on OS than on PFS,[7,28] which is in

Table 3. Multivariate model of the impact of prognostic factors for PFS and OS incorporating the MRI-based score (MPSS). The model was calculated using the MPSS based on either the cut-off for wbMRI FL (top) or axMRI FL (bottom).

	Whole-body MPSS-based model					
		PFS			OS	
Parameter	HR	95%-CI	*P* value	HR	95%-CI	*P* value
wb-MPSS stage II	2.19	1.32 – 3.65	0.003	2.37	0.88 – 6.39	0.09
wb-MPSS stage III	3.65	1.90 – 7.01	<0.001	5.19	1.65– 16.34	0.005
ISS (II *vs.* I)	1.12	0.69 – 1.84	0.64	0.75	0.33 – 1.69	0.48
ISS (III *vs.* I)	1.43	0.86 – 2.39	0.16	1.97	0.96 – 4.04	0.06
LDH (>ULN)	1.01	0.64 – 1.60	0.95	1.79	0.95 – 3.38	0.07
Adverse cytogenetics	1.60	1.08 – 2.39	0.02	2.07	1.05 – 4.08	0.04
Induction therapy without novel agents	1.01	0.70 - 1.48	0.94	1.80	0.98 - 3.31	0.06
	Axial MPSS-based model					
		PFS			OS	
Parameter	HR	95%-CI	*P* value	HR	95%-CI	*P* value
ax-MPSS stage II	2.27	1.36 – 3.80	0.002	2.02	0.76 – 5.39	0.16
ax-MPSS stage III	3.95	1.94 – 8.03	<0.001	5.73	1.79– 18.33	0.003
ISS (II *vs.* I)	1.18	0.72 – 1.92	0.51	0.76	0.34 – 1.73	0.51
ISS (III *vs.* I)	1.34	0.78 – 2.30	0.28	1.77	0.83 – 3.76	0.14
LDH (>ULN)	1.06	0.67 – 1.69	0.79	2.04	1.07 – 3.89	0.03
Adverse cytogenetics	1.59	1.07 – 2.36	0.02	2.01	1.02 – 3.95	0.04
Induction therapy without novel agents	0.97	0.67 - 1.40	0.86	1.70	0.93 - 3.10	0.08

line with our results, this might be impeded by the sample size of our cohort. Furthermore, previously described correlations between higher ISS stages and DI[8,19] might weaken the effects of these factors in our multivariate analyses.

The information summarized in the MPSS can be determined rapidly in clinical routine and the MPSS can therefore be calculated without significant additional effort by the radiologist (Table 2). Allocation to different stages is not affected by the examination technique (wbMRI or axMRI) (*Online Supplementary Table S3*) and the discrimination between the three stages works reliably (Figure 3).

MPSS stage I identified patients at low risk, whose median OS had not been reached at time of the present analysis. In our multivariate model, stage II was an independent risk factor for an adverse PFS (wb/axMRI: HR=2.19/2.27) whereas stage III was associated with a poor PFS (wb/axMRI: HR=3.65/3.95) and OS (wb/axMRI: HR=5.19/5.73). Moreover, stage III, together with adverse cytogenetics (wb/axMRI: HR=2.07/2.01), remained the only consistent, statistically significant independent prognostic risk factors for shortened OS (Table 3). This underscores the importance of an additional evaluation of MRI.

Providing information on plasma cell infiltration (DI and FL patterns) in a large volume of bone marrow, MRI complements CT, whose chief strength is to detect destruction of mineralized bone.[15,29] The current study supports the use of MRI in clinical routine in addition to CT for newly diagnosed, symptomatic MM since it shows that MRI adds significant information on prognosis and treatment necessity.[14]

In comparison to other prognostic scores such as the ISS[3], MRI provides additional clinical information, e.g. on extramedullary disease and spinal cord compression. As previously described, MRI can be repeated after key therapeutic steps to reassess prognosis and treatment response independently of serological markers.[20,30]

The issue of whether PET-CT rather than MRI should be used in monoclonal plasma cell diseases for assessment of bone marrow infiltration and extramedullary disease has not been clarified yet. MRI seems to be superior at initial staging due to its high sensitivity for both FL and DI, whereas PET-CT provides information on metabolic activity and therefore helps to assess treatment response early and more precisely.[31,32]

Two articles by Moulopoulos *et al.*[8,10] described that DI assessed by MRI correlates with adverse cytogenetics, higher ISS, anemia and increased biomarkers of angiogenesis. This might partially explain the poor prognosis associated with moderate/severe DI. More than seven FL are associated with lowered serum albumin and higher levels of LDH, C-reactive protein and creatinine.[9] In another study, the presence of FL was associated with a higher number of osteolytic lesions than moderate/severe or minimal DI.[8] No correlation was seen between bone marrow plasmacytosis, hemoglobin value or adverse cytogenetics.[8,9] A further analysis of these connections might advance the understanding of the pathophysiology of different MRI patterns in MM.

The limitations of the current study are its retrospective nature and the fact that it was conducted in a single center. In addition, there was no stratification of patients according to induction and/or maintenance therapies. A further validation of the score in independent cohorts is planned.

In summary, our study demonstrated that both DI pattern and FL number have a significant impact on PFS and OS. Minimal and S&P DI are favorable patterns, whereas moderate and severe DI are unfavorable ones. The prognosis becomes increasingly worse with a higher number of FL without a distinct cut-off. However, an arbitrary cut-off value at the highest quartile (>25 FL in wbMRI and

>7 FL in axMRI) allows a reliable prognostic discrimination with reasonable effort for the radiologist. The combination of these patterns led to the development of a prognostic scoring system (MPSS), for both wbMRI and axMRI, to predict PFS and OS in transplant-eligible MM patients. The information provided by MPSS adds sensibly to established factors such as adverse cytogenetics.

Acknowledgments

The authors thank all participating patients and their families.

Funding

This retrospective analysis was funded in part by the Dietmar Hopp-Foundation and by the German Federal Ministry of Education and Research (BMBF) within the framework of the e:Med research and funding concept (grant # 01ZX1309A).

Authorship and Disclosures

Information on authorship, contributions, and financial & other disclosures was provided by the authors and is available with the online version of this article at www.haematologica.org.

References

1. Palumbo A, Anderson K. Multiple myeloma. N Engl J Med. 2011;364 (11):1046-1060.
2. Kumar SK, Dispenzieri A, Lacy MQ, et al. Continued improvement in survival in multiple myeloma: changes in early mortality and outcomes in older patients. Leukemia. 2014;28(5):1122-1128.
3. Greipp PR, San Miguel J, Durie BGM, et al. International staging system for multiple myeloma. J Clin Oncol. 2005;23(15):3412-3420.
4. Walker BA, Leone PE, Chiecchio L, et al. A compendium of myeloma-associated chromosomal copy number abnormalities and their prognostic value. Blood. 2010;116 (15):e56-65.
5. Neben K, Lokhorst HM, Jauch A, et al. Administration of bortezomib before and after autologous stem cell transplantation improves outcome in multiple myeloma patients with deletion 17p. Blood. 2012; 119(4):940-948.
6. Moreau P, Cavo M, Sonneveld P, et al. Combination of International Scoring System 3, high lactate dehydrogenase, and t(4;14) and/or del(17p) identifies patients with multiple myeloma (MM) treated with front-line autologous stem-cell transplantation at high risk of early MM progression–related death. J Clin Oncol. 2014;32(20):2173-2180.
7. Neben K, Jauch A, Bertsch U, et al. Combining information regarding chromosomal aberrations t(4;14) and del(17p13) with the International Staging System classification allows stratification of myeloma patients undergoing autologous stem cell transplantation. Haematologica. 2010;95 (7):1150-1157.
8. Moulopoulos LA, Dimopoulos MA, Kastritis E, et al. Diffuse pattern of bone marrow involvement on magnetic resonance imaging is associated with high risk cytogenetics and poor outcome in newly diagnosed, symptomatic patients with multiple myeloma: a single center experience on 228 patients. Am J Hematol. 2012;87(9):861–864.
9. Walker R, Barlogie B, Haessler J, et al. Magnetic resonance imaging in multiple myeloma: diagnostic and clinical implications. J Clin Oncol. 2007;25(9):1121-1128.
10. Moulopoulos LA, Dimopoulos MA, Christoulas D, et al. Diffuse MRI marrow pattern correlates with increased angiogenesis, advanced disease features and poor prognosis in newly diagnosed myeloma treated with novel agents. Leukemia. 2010; 24(6):1206-1212.
11. Dimopoulos MA, Hillengass J, Usmani S, et al. Role of magnetic resonance imaging in the management of patients with multiple myeloma: a consensus statement. J Clin Oncol. 2015;33(6):657-664.
12. Moulopoulos LA, Dimopoulos MA. Magnetic resonance imaging of the bone marrow in hematologic malignancies. Blood. 1997;90(6):2127-2147.
13. Ludwig H, Tscholakoff D, Neuhold A, Frühwald F, Rasoul S, Fritz E. Magnetic resonance imaging of the spine in multiple myeloma. Lancet. 1987;330(8555):364-366.
14. Rajkumar SV, Dimopoulos MA, Palumbo A, et al. International Myeloma Working Group updated criteria for the diagnosis of multiple myeloma. Lancet Oncol. 2014;15 (12):e538-548.
15. Dimopoulos M, Terpos E, Comenzo RL et al. International Myeloma Working Group consensus statement and guidelines regarding the current role of imaging techniques in the diagnosis and monitoring of multiple Myeloma. Leukemia. 2009;23(9):1545-1556.
16. Merz M, Hielscher T, Wagner B, et al. Predictive value of longitudinal whole-body magnetic resonance imaging in patients with smoldering multiple myeloma. Leukemia. 2014;28(9):1902-1908.
17. Hillengass J, Weber M-A, Kilk K, et al. Prognostic significance of whole-body MRI in patients with monoclonal gammopathy of undetermined significance. Leukemia. 2014;28(1):174-178.
18. Hillengass J, Fechtner K, Weber M-A, et al. Prognostic significance of focal lesions in whole-body magnetic resonance imaging in patients with asymptomatic multiple myeloma. J Clin Oncol. 2010;28(9):1606-1610.
19. Moulopoulos LA, Gika D, Anagnostopoulos A, et al. Prognostic significance of magnetic resonance imaging of bone marrow in previously untreated patients with multiple myeloma. Ann Oncol. 2005;16(11):1824-1828.
20. Hillengass J, Ayyaz S, Kilk K, et al. Changes in magnetic resonance imaging before and after autologous stem cell transplantation correlate with response and survival in multiple myeloma. Haematologica. 2012;97(11): 1757-1760.
21. Bäuerle T, Hillengass J, Fechtner K, et al. Multiple myeloma and monoclonal gammopathy of undetermined significance: importance of whole-body versus spinal MR imaging. Radiology. 2009;252(2):477-485.
22. Baur A, Stäbler A, Nagel D, et al. Magnetic resonance imaging as a supplement for the clinical staging system of Durie and Salmon? Cancer. 2002;95(6):1334-1345.
23. Stäbler A, Baur A, Bartl R, Munker R, Lamerz R, Reiser MF. Contrast enhancement and quantitative signal analysis in MR imaging of multiple myeloma: assessment of focal and diffuse growth patterns in marrow correlated with biopsies and survival rates. AJR Am J Roentgenol. 1996;167(4):1029-1036.
24. Holm S. A simple sequentially rejective multiple test procedure. Scand J Statist. 1979;6 (2):65-70.
25. Harrell FE. Regression modeling strategies: with applications to linear models, logistic regression, and survival analysis. Heidelberg: Springer Heidelberg, Germany; 2011.
26. Andrulis M, Bäuerle T, Goldschmidt H, et al. Infiltration patterns in monoclonal plasma cell disorders: correlation of magnetic resonance imaging with matched bone marrow histology. Eur J Radiol. 2014;83(6):970-974.
27. Ricci C, Cova M, Kang YS, et al. Normal age-related patterns of cellular and fatty bone marrow distribution in the axial skeleton: MR imaging study. Radiology. 1990;177 (1):83-88.
28. Sonneveld P, Schmidt-Wolf IGH, van der Holt B, et al. Bortezomib induction and maintenance treatment in patients with newly diagnosed multiple myeloma: results of the randomized phase III HOVON-65/ GMMG-HD4 trial. J Clin Oncol. 2012;30 (24):2946-2955.
29. Caers J, Withofs N, Hillengass J, et al. The role of positron emission tomography-computed tomography and magnetic resonance imaging in diagnosis and follow up of multiple myeloma. Haematologica. 2014;99(4): 629-637.
30. Moulopoulos LA, Dimopoulos MA, Alexanian R, Leeds NE, Libshitz HI. Multiple myeloma: MR patterns of response to treatment. Radiology. 1994;193(2):441-446.
31. Spinnato P, Bazzocchi A, Brioli A, et al. Contrast enhanced MRI and 18F-FDG PET-CT in the assessment of multiple myeloma: A comparison of results in different phases of the disease. Eur J Radiol. 2012;81(12): 4013-4018.
32. Zamagni E, Nanni C, Patriarca F, et al. A prospective comparison of 18F-fluorodeoxyglucose positron emission tomography-computed tomography, magnetic resonance imaging and whole-body planar radiographs in the assessment of bone disease in newly diagnosed multiple myeloma. Haematologica. 2007;92(1):50-55.